III.D.2 Analysis of Percent On-Cell Reformation of Methane in Solid Oxide Fuel Cell Stacks: Thermal, Electrical, and Stress Analysis

Objectives

- Quantify the effect of varying the percentage of the steam-methane reformation reaction occurring on-cell on the thermal, electrical, and mechanical performance of a generic SOFC stack design.
- Determine the optimal on-cell reformation percentage.
- Demonstrate - with simulations of stack operation - how the optimal methane fuel mixture can be used to improve stack performance.

Accomplishments

- Discovered that at least 40% of the steam-methane reformation reaction could be performed on-cell for cross-flow and counter-flow stacks of 10x10 cm and 20x20 cm cell sizes.
- Identified that at least 80% of the steam-methane reformation reaction could be performed on-cell for co-flow configuration stacks because the stack performance improved continuously with increasing percent on-cell reformation.
- Demonstrated that the thermal and mechanical performance could be manipulated with on-cell reformation without adverse effects to the electrical performance of the stack.

Introduction

The solid oxide fuel cell (SOFC) industry continues to develop larger, more powerful cell stacks for stationary power applications, and thermal management remains a critical issue for the reliable operation of these stacks. On-cell steam-methane reformation is an effective means of removing excess heat generated within large SOFC stacks. The endothermic reformation reaction, when employed directly on the anode, immediately removes excess heat generated by the electrochemical oxidation reactions. Thus on-cell reformation (OCR) is attractive because of the decreased thermal load it can provide as well as the cost benefits of decreased reformer and heat exchanger size. The challenge presented by OCR is related to the rapid kinetics of the reformation reaction on a standard Ni-YSZ anode. With increasing percent OCR, the resultant endotherm can cause a significant local temperature depression near the fuel inlet on the anode. Cooling near the fuel inlet and subsequently increased heating downstream due to increased hydrogen concentration and electrical current density can create a large difference between the minimum and maximum temperatures on the cell (ΔT). Along with the cell ΔT there can be an increase in the thermal stresses on the anode creating an unreliable condition for cell operation. This study was performed to analyze the effect of various percent OCR on the thermal, electrical, and mechanical performance of typical planar SOFC designs with 10x10- and 20x20-cm active cell areas.

Mohammad A. Khaleel (Primary Contact), Kurt Recknagle, Brian Koeppel, Xin Sun, John Vetrano, and Sato Yokuda
Pacific Northwest National Laboratory (PNNL)
902 Battelle Blvd.
Richland, WA 99352
Phone: (509) 375-2438; Fax: (509) 375-4392
E-mail: moe.khaleel@pnl.gov

DOE Project Manager: Travis Shultz
Phone: (304) 285-1370
E-mail: Travis.Shultz@netl.doe.gov

Approach

A computational modeling tool for simulating the multi-physics of SOFC operation was used in this study. The PNNL-developed SOFC-MP code solves the equations for mass transport, energy, and electrochemistry required to predict the fluid flow, temperature, species, and current density distributions in a three-dimensional SOFC geometry [1,2,3]. The 3-dimensional model geometries and boundary conditions were similar to those of earlier work by this group [4]. The electrochemistry model used was described by Chick et al. [5], calibrated for application to planar stack simulations [6,7], and updated to provide an improved anode concentration polarization model [8]. The steam-methane reformation model was described by Recknagle et al. [9] and revised to include a 1st order Arrhenius rate expression derived experimentally at PNNL [10].

In the study it was assumed the unreformed fuel mixture containing methane, steam, and nitrogen passed through a fuel stream pre-heater to an external reformer where various percentages of the methane were reacted using excess steam in a steam-to-carbon ratio of 2. The anode input gas mixture was then determined based on the water-gas-shift reaction equilibrium at 750°C. This study examined fuels with compositions representing 0 to 80% OCR as summarized in Table 1.

TABLE 1. Molar Compositions of Fuel Mixtures Supplied from External Reformer to the Stack

% OCR	H_2	CO	H_2O	CO_2	CH_4	N_2
0	0.538	0.127	0.181	0.052	0.000	0.101
20	0.465	0.096	0.232	0.059	0.039	0.109
40	0.376	0.064	0.295	0.062	0.084	0.118
60	0.264	0.033	0.377	0.058	0.137	0.129
80	0.118	0.008	0.488	0.042	0.202	0.142

In the simulations, the iterative solutions for all cases were well converged with respect to mass, momentum, energy, chemistry, and electrochemistry. For these analyses, the electrochemical performance of a cell operating on the fully pre-reformed fuel was taken to be 0.60 A/cm^2 at 0.68 volts and 75% fuel utilization, at an average cell temperature of 750°C. All solutions used adjustable inflow temperature and cell voltage to achieve an average cell temperature of 750°C and current density of 0.6 A/cm^2, respectively. Because all cases simulated stack operation at the same average temperature and current density except for variations in the output power, the differences in net heat load were attributable to the heat removed by OCR. Subsequently, the thermal performance of each stack could be compared directly. Two air flow rates were used to examine the air cooling effect at 30% and 15% air utilization.

After the electrochemical-thermal solution was obtained, the resulting temperature profile was used as the thermal load in the subsequent structural analysis to calculate stresses in the cell. The maximum principal stress of the anode was then obtained for each of the cases. For the structural evaluation, minimal displacement support boundary conditions were used at the bottom of the cell. These simplified boundary conditions do not constrain the unit cell model as completely as if it was within a full stack, and are suitable for direct case-to-case comparisons of the stress in a trend analysis as is presented here.

Results

Figure 1 shows the cell ΔT (triangular icons), and the maximum principal stress (S1) in the anode (red square or green "x" icons) for the 10x10-cm counter-flow stack as a function of percent OCR. The scale for the cell ΔT is on the left of the figure and the scale for the stress on the right. With 30% air utilization, cell ΔT for this stack varied between 45° and 85°C with a minimum at 40% OCR. The anode stress followed the trend of ΔT closely also reaching a minimum value at 40% OCR for 30% air use. As shown by the green curve in Figure 1, when more air was supplied to the stack (15% air use) the variation of stress was decreased,

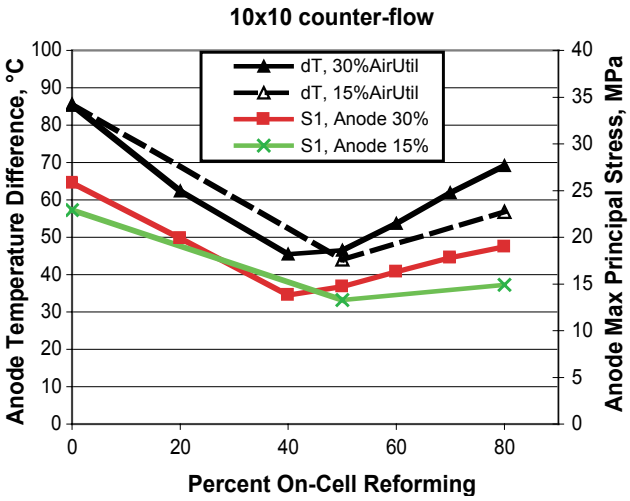

FIGURE 1. Cell Temperature Difference (ΔT) and Maximum Principal Stress (S1) versus % OCR for 10x10-cm Counter-Flow Cases

but the magnitude of the stress was not decreased substantially. For both air utilizations, the anode stress was at least 14 MPa.

Table 2 summarizes cases for each stack configuration and cell size with 30% and 15% air use, and the percent OCR in which the anode stress was minimum, including the data point representing the 10x10 cm counter-flow stack described in Figure 1. The 10x10-cm cross-flow stack results were similar to the counter-flow results featuring a minimum anode stress and ΔT at intermediate OCR (50%) with 30% air use. With more cathode air (15% air use) neither the maximum temperature nor the anode stresses were significantly reduced. The 10x10-cm co-flow stack results, with 30% air use, showed little change to the magnitude of ΔT and a slight decrease of anode stress for increasing percent OCR. The co-flow stack also showed a benefit from increased cathode air (15% air use) in the form of decreased ΔT and stress over the full range of percent OCR. Stresses in the anode were similar in magnitude to those predicted for the counter- and cross-flow stacks with a minimum value of approximately 15 MPa. Gross electrical power density of 0.4 W/cm^2 was virtually unaffected for each of the 10x10-cm stacks.

Cell ΔT and anode stresses were substantially larger in the 20x20-cm stack simulation results than those of the 10x10-cm cases. Similar to the 10x10-cm cases, the anode stresses were minimum values at intermediate percent OCR for 30% air use in cross- and counter-flow configurations. With 15% air use the cross and counter-flow stacks benefited most from 0% OCR while the co-flow stack had decreased stress, ΔT, and maximum temperature at 80% OCR. In each 20x20-cm case the electrical power density deviated little from the nominal value of 0.4 W/cm^2.

TABLE 2. Summary of Results and Related %OCR with Minimum Anode Stress

Cell Size / Air Use, %	Flow Configuration	% OCR	Temperature, °C		Anode Stress S1max, MPa	Power, W/cm^2
			Maximum	ΔT		
10x10 / 30%	Cross	50	775	74	14.2	0.403
	Co-flow	80	779	74	17.2	0.403
	Counter	40	768	45	13.8	0.405
10x10 / 15%	Cross	50	774	66	14.0	0.405
	Co-flow	80	777	66	14.8	0.403
	Counter	50	768	44	13.3	0.406
20x20 / 30%	Cross	50	866	241	60.2	0.399
	Co-flow	80	844	178	40.0	0.403
	Counter	60	832	196	71.7	0.409
20x20 / 15%	Cross	0	851	191	45.2	0.397
	Co-flow	80	817	124	25.5	0.404
	Counter	0	851	188	45.4	0.415

Conclusions

- The analyses showed that the anode stress achieved local minima along with the temperature difference on the cell with 40 to 50% OCR in counter-flow and cross-flow stacks of 10x10-cm size.
- Unlike the cross-flow and counter-flow stacks, the co-flow stack showed substantial thermal benefit due to increased air flow (15% air utilization) as the anode stress and cell temperature difference was decreased over the full range of OCR.
- Within the 20x20-cm cases the co-flow configuration stack had the smallest anode stresses and cell temperature difference, both of which were continuously decreased with increasing OCR.
- Gross electrical power density of 0.4 W/cm^2 was virtually unaffected for each 10x10-cm case; little power density variation was predicted in the 20x20-cm cases as well.
- For the conditions and particular generic stacks of this study, the results suggest 40 to 50% reformation on-cell should be considered for cross-flow and counter-flow stacks, and OCR as high as 80% with at most 15% air utilization should be desirable in co-flow stacks.

Future Directions

- Modeling will be performed in support of experiments to modify anode material providing optimal anode activity for thermal performance.
- Optimize the thermal, mechanical, and electrical performance of stacks of larger size and varying design.

FY 2006 Publications/Presentations

1. Recknagle KP, ST Yokuda, DT Jarboe, and MA Khaleel. 2006. *Analysis of Percent On-Cell Reformation in SOFC Stacks: Thermal, Electrical, and Stress Analysis*. SECA Topical Report.

2. Recknagle KP, DT Jarboe, DL King, MA Khaleel, and P Singh. 2005. *Modeling of On-Cell Reformation in SOFC Stacks: The Effect of Methane Conversion Activity Manipulations on Stack Performance*. SECA Topical Report.

3. Recknagle KP, DT Jarboe, KI Johnson, VN Korolev, MA Khaleel, and P Singh. 2005. *Electrochemistry And On-Cell Reformation Modeling For Solid Oxide Fuel Cell Stacks*. 30th International Conference & Exposition on Advanced Ceramics and Composites, Cocoa Beach FL, January 24, 2006.

4. Khaleel MA, KP Recknagle, JS Vetrano, X Sun, BJ Koeppel, KI Johnson, VN Korolev, BN Nguyen, AM Tartakovsky, and P Singh. Recent Development of Modeling Activities at PNNL. SECA Core Technology Program Peer Review, Lakewood, CO, October 25-26, 2005.

References

1. Khaleel MA. 2005. "Finite Element SOFC Analysis with SOFC-MP and MSC.Marc/Mentat-FC." Proceedings of the Sixth Annual SECA Workshop. National Engineering Technology Laboratory, Morgantown, West Virginia.

2. Khaleel MA, Z Lin, P Singh, W Surdoval, and D Collins. 2004. "A Finite Element Analysis Modeling Tool for Solid Oxide Fuel Cell Development: Coupled Electrochemistry, Thermal, and Flow Analysis in Marc." J. Power Sources, 130(1-2):136-148.

3. Recknagle KP, RE Williford, LA Chick, DR Rector, and MA Khaleel. 2003. "Three-dimensional thermo-fluid electrochemical modeling of planar SOFC stacks." J. Power Sources, 113:109-114.

4. Recknagle KP, DT Jarboe, DL King, MA Khaleel, and P Singh. 2005. Modeling of On-Cell Reformation in SOFC Stacks: The Effect of Methane Conversion Activity Manipulations on Stack Performance. PNNL-15311, Pacific Northwest National Laboratory, Richland, Washington.

5. Chick LA, JW Stevenson, KD Meinhardt, SP Simner, JE Jaffe, and RE Williford. 2000. "Modeling and Performance of Anode-Supported SOFC." 2000 Fuel Cell Seminar – Abstracts, pp. 619-622.

6. Chick LA, RE Williford, JW Stevenson, CF Windisch Jr, and SP Simner. 2002. "Experimentally-Calibrated, Spreadsheet-Based SOFC Unit-Cell Performance Model." 2002 Fuel Cell Seminar - Abstracts.

7. Keegan K, M Khaleel, L Chick, K Recknagle, S Simner, and J Deibler. 2002. "Analysis of a Planar Solid Oxide Fuel Cell-Based Automotive Auxiliary Power Unit." Society of Automotive Engineers, Congress 2002 Proceedings, 2002-01-0413.

8. Williford RE, LA Chick, GD Maupin, SP Simner, and JW Stevenson. 2003. "Diffusion Limitations in the Porous Anodes of SOFCs." J. Electrochemical Soc. 150(8): A1067-A1072.

9. Recknagle KP, P Singh, LA Chick, and MA Khaleel. 2004. "Modeling of SOFC Stacks with On-Cell Steam-Methane Reformation at PNNL." PNNL-SA-43248, Proceedings of the Fuel Cell 2004 Seminar, San Antonio, Texas.

10. King DL, Y Wang, Y Chin, Y Lin, H Roh, and R Romiarek. 2005. "Controlling Activity and Stability of Ni-YSZ Catalysts for On-Anode Reforming." Presented at SECA Core Technology Program Review Meeting, Tampa, Florida.